

Cross-Coupling of NHC/CAAC-Based Carbodicarbene: Synthesis of Electron-Deficient Diradicaloids

Vasu Malhotra, Benedict J. Elvers, Ramapada Dolai, Nicolas Chrysochos, Siva Sankar Murthy Bandaru, Tejaswinee Gangber, Neethinathan Johnee Britto, Ivo Krummenacher, Gopalan Rajaraman,* Holger Braunschweig,* Carola Schulzke,* and Anukul Jana*



Cite This: *J. Am. Chem. Soc.* 2024, 146, 29481–29490



Read Online

ACCESS |



Metrics & More

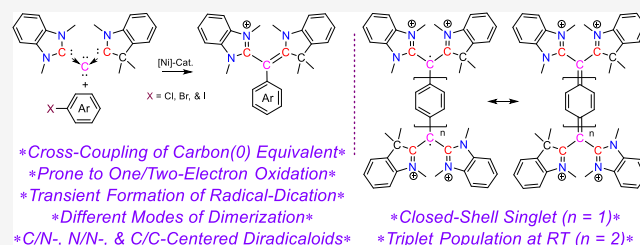


Article Recommendations



Supporting Information

ABSTRACT: Herein, we report nickel(0)-catalyzed cross-coupling reactions of NHC/CAAC-based carbodicarbene (NHC = *N*-heterocyclic carbene and CAAC = cyclic(alkyl)(amino)carbene) with different aryl chlorides, bromides, and iodides. The resulting aryl-substituted cationic carbodicarbene derivatives are prone to one-electron oxidation yielding radical-dications, which, depending on the aryl motif employed, follow different modes of radical–radical dimerization and constitute an entry point to carbon/nitrogen- and nitrogen/nitrogen-centered diradicaloids. Subsequently, this coupling strategy was strategically applied to the synthesis of *p*-phenylene- and *p,p'*-biphenylene-bridged carbon/carbon-centered electron-deficient diradicaloids. The employed π -conjugated spacer plays a crucial role in determining the triplet population at room temperature by modulation of the singlet–triplet gap: EPR inactive for *p*-phenylene vs EPR active for *p,p'*-biphenylene. Nearly two decades after the disclosure of carbodicarbenes as donor-stabilized atomic carbon equivalents by Tonner and Frenking in 2007, we demonstrate their cross-couplings with a series of aryl halides/dihalides and, based on this, developed a modular methodology for the systematic synthesis of various electron-deficient diradicaloids.



INTRODUCTION

Transition metal-catalyzed cross-coupling reactions between functionalized aryl compounds have been, and still are, critically important in the synthesis of a variety of functional molecules ranging from pharmaceuticals to polymers (I, Scheme 1).¹ Such cross-coupling reactions were also known for the buildup of various alkyl-, vinyl-, and alkynyl-functional molecules.² Furthermore, carbon(II)-centers of *N*-heterocyclic carbenes (NHCs) were coupled to various aryl halides, resulting in the formation of (dihydro)-imidazolium cations (II, Scheme 1), which were then utilized as synthons for the generation of radicals under one-electron reduction.³ Following the discovery of the concept of carbodicarbene as a donor-stabilized atomic carbon equivalent,⁴ various functionalizations of carbodicarbenes have been reported, primarily harnessing the nucleophilic properties of the carbon(0)-center.⁵ These findings inspired us to investigate the feasibility of cross-coupling reactions of the carbonic carbon(0)-center. Herein, the successful cross-coupling of an NHC/CAAC-based carbodicarbene (NHC = *N*-heterocyclic carbene and CAAC = cyclic(alkyl)(amino)carbene)⁶ with different aryl chlorides, bromides, and iodides is reported (III, Scheme 1). The resulting aryl-functionalized cationic carbodicarbene derivatives are able to undergo one-electron oxidation under the formation of radical-dications, which then follow different modes of radical–radical dimerization based on the nature of

the aryl groups employed. Furthermore, we also considered the use of π -conjugated diiodoaryls as coupling partners, and the resulting dicationic bis-carbodicarbene derivatives undergo reversible two-electron oxidation, yielding electron-deficient diradicaloids. Please note that NHC/CAAC-based carbodicarbene can be depicted in various forms A–D, considering different concepts of bonding and representation (Scheme 1).⁷ We have opted to represent it here as the mono-zwitterionic form C by taking into account the different electronic natures of NHC and CAAC; specifically, NHC is relatively less nucleophilic and less electrophilic in nature than CAAC,⁸ which is also reflected in the solid-state molecular structure of NHC/CAAC-based carbodicarbene.⁶

RESULTS AND DISCUSSION

The cross-coupling reactions of NHC/CAAC-based carbodicarbene I with phenyl chloride/bromide/iodide or 4-*tert*-butyl-phenyl bromide/iodide in the presence of a catalytic amount of Ni(COD)₂/PPh₃ led to the isolation of yellow

Received: July 1, 2024

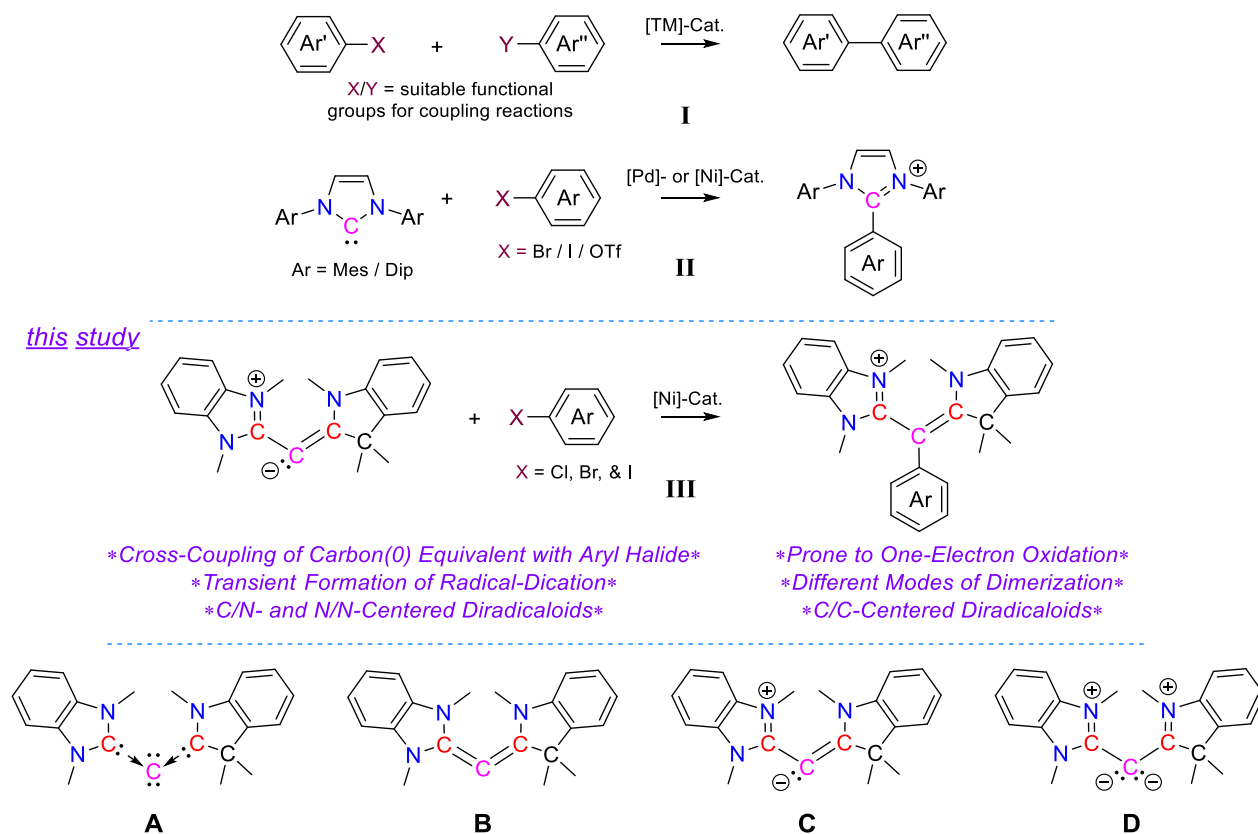
Revised: October 2, 2024

Accepted: October 3, 2024

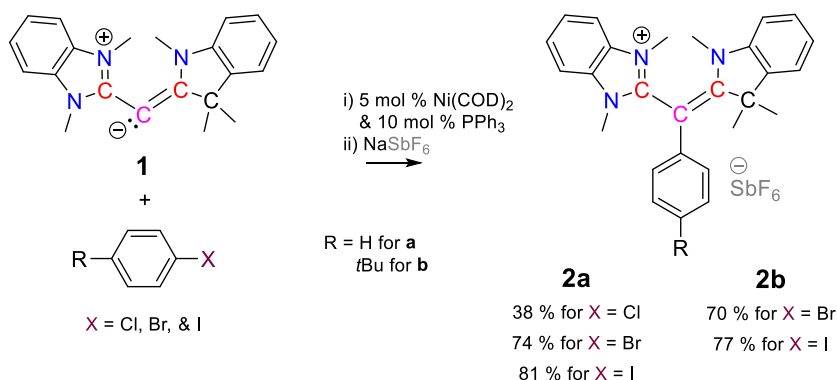
Published: October 19, 2024



Scheme 1. Schematic Representation of Reactions I–III (Corresponding Counter Anions of Ionic Compounds Are Omitted for Clarity) and Four Possible Representations of NHC/CAAC-Based Carbodicarbene A–D



Scheme 2. Synthesis of 2a/2b



crystalline **2a/2b** (Scheme 2).⁹ In the $^{13}\text{C}\{^1\text{H}\}$ NMR spectra of **2a** and **2b**, the resonances at $\delta = 88.80$ and 88.66 ppm are assigned to the aryl-functionalized carbonic carbon, respectively. The single-crystal X-ray diffraction analyses of **2a** and **2b** reveal that the C1–C3 bond lengths ($1.454(4)/1.436(5)$ Å) are longer than the C1–C2 distance ($1.368(4)/1.363(5)$ Å), reflecting the different electronic natures of NHC and CAAC (Figure 1).

With cyclic voltammetry, it was shown that both compounds **2a** and **2b** are prone to oxidation at $E_{1/2} = 0.71$ ¹⁰ and 0.58 V vs Fc/Fc^+ , respectively (Figure 2).

Subsequent chemical oxidation of **2a/2b** with $[\text{NO}][\text{SbF}_6]$ in CH_3CN led to an immediate visible color change from yellow to blue and red, respectively. In the case of **2a**, compound **4** was obtained along with its two-electron oxidized form **5** (Scheme 3). The formation of **4/5** indicates that the

initially formed radical-dication **3a** undergoes heteroleptic dimerization¹¹ between the *para*-position of the phenyl group and the *para*-position of the benzannulated CAAC-motif (relative to the *N*-substituent). This dimerization is also supported by the spin-density analysis of **3a** at the UB3LYP-D3/Def2-SVP($\text{CH}_3\text{CN-SMD}$) level of theory,⁹ which indicates that the unpaired spin is mostly delocalized over the carbonic carbon, *ortho*- and *para*-positions of the phenyl group, and nitrogen/benzene-ring (*ortho*- and *para*-positions with respect to the *N*-substituent) of the CAAC-motif (Figure 3 - left). Reduction of the crude reaction mixture with elemental zinc led to the pure crystalline compound **4** in 28% yield. The single-crystal X-ray diffraction analysis unambiguously confirmed the formation of **4**, proving the bond-connectivity to be the result of heteroleptic dimerization of radical-dication **3a** (Figure 4).

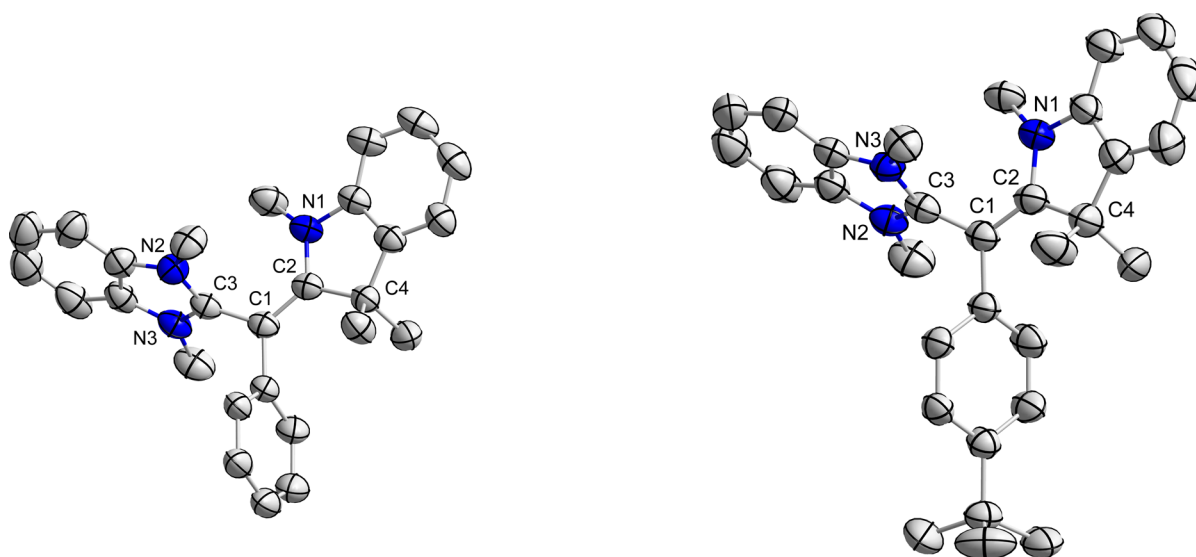


Figure 1. Molecular structures of **2a** and **2b** at 40 and 50% probability levels, respectively. All hydrogens and counteranions are omitted for clarity. Selected bond lengths (Å) and bond angles (°) for **2a**: C1–C2 1.368(4), C1–C3 1.454(4), C1–C5 1.534(11); C2–C1–C3 121.8(2), C2–C1–C5 125.7(12), C3–C1–C5 111.5(11); and for **2b**: C1–C2 1.363(5), C1–C3 1.436(5), C1–C5 1.502(5); C2–C1–C3 120.9(3), C2–C1–C5 124.3(3), C3–C1–C5 114.7(3).

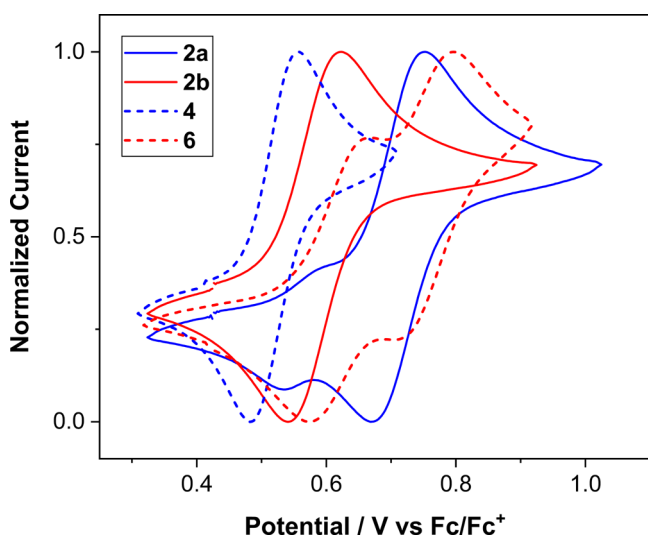


Figure 2. Cyclic voltammograms of **2a**, **2b**, **4**, and **6** at a 100 mV/s scan rate in CH₃CN (0.1 mol/L Bu₄NPF₆) at room temperature.

A cyclic voltammetry study confirmed that compound **4** can be subjected to a single two-electron oxidation at $E_{1/2} = 0.52$ V vs Fc/Fc⁺ (Figure 2), resulting in the formation of tetracation **5**; this also supports the co-formation of **5** along with the initially formed **4** during the oxidation of **2a** using [NO][SbF₆] ($E_{1/2} = 0.87$ V vs Fc/Fc⁺ in CH₃CN).¹² Subsequent chemical oxidation of **4** with two equivalents of [NO][SbF₆] indeed leads to **5**.¹³ The UV/vis/NIR spectrum of the solution resulting from the chemical oxidation shows the longest wavelength absorption at $\lambda_{\max} = 686$ nm for **5** (Figure S47), which is considerably red-shifted in comparison to that of **4** ($\lambda_{\max} = 393$ nm) (Figure S41). However, due to its limited stability in CH₃CN, it could not be crystallized, even after several attempts.

In the case of **2b**, compound **6** was obtained along with its one- and two-electron oxidized compounds **7** and **8**, respectively (Scheme 4). The formation of **6/7/8** indicates

that the initially formed radical-dication **3b** undergoes homoleptic dimerization¹⁴ between the *para*-positions of the benzannulated CAAC-motif (relative to the *N*-substituent). This is also supported by the spin density plot⁹ of **3b**, in which the unpaired spin is delocalized as in the case of **3a** (Figure 3 - right); however, here the *t*Bu-substituent blocks the *para*-position carbon of the phenyl group from partaking in the dimerization. The strikingly distinct modes of dimerization observed for radical-dications **3a** and **3b** are hence defined by the *para*-substituent of the phenyl ring: H vs *t*Bu. Such kind of substituent-dependent dimerization mode is well-known in the case of triarylmethyl radicals.¹⁵ From the crude reaction mixture, radical-trication **7** was obtained after the workup. Compound **7** exhibits a broad EPR signal with unresolved hyperfine couplings, reflecting a highly delocalized spin system (Figure S133). Subsequently, compound **6** can be isolated by the reduction of **7** with elemental zinc. Compound **6** undergoes two separate one-electron oxidations at $E_{1/2} = 0.62$ and 0.75 V vs Fc/Fc⁺ (Figure 2), resulting in the sequential formation of radical-trication **7** and tetracation **8**;¹⁶ this also supports the co-formation of **7** and **8** along with the initially formed **6** during the oxidation of **2b** with [NO][SbF₆]. Compounds **6/7/8** exhibit the longest wavelength absorptions in their UV/vis/NIR spectra at $\lambda_{\max} = 412$ ($\epsilon = 38200$ L mol⁻¹cm⁻¹), 1510 ($\epsilon = 36700$ L mol⁻¹cm⁻¹), and 896 nm, respectively (Figure S61). Single-crystal X-ray analyses of **6/7/8**¹⁷ unambiguously confirmed their formation, corroborating the bond-connectivity and, hence, homoleptic dimerization of radical-dication **3b** (Figures 5, S87, and S88). The bond distance between the two phenylene rings of the central *p*-biphenylene bridge gradually decreases from 1.498(7) to 1.460(10) to 1.431(12) Å, indicating a progressive development of double-bond character upon sequential oxidation.

Subsequently, to realize the tetracationic Thiele's¹⁸ and Chichibabin's¹⁹ hydrocarbon analogues of carbon-centered diradicaloids, the cross-coupling reactions of NHC/CAAC-based carbodicarbene **1** were strategically performed with 1,4-diiodobenzene and 4,4'-diiodobiphenyl in the presence of catalytic amounts of Ni(COD)₂/PPh₃, obtaining **9a/9b** in 75

Scheme 3. Oxidation of 2a

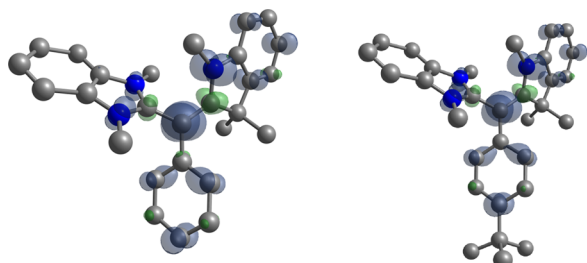
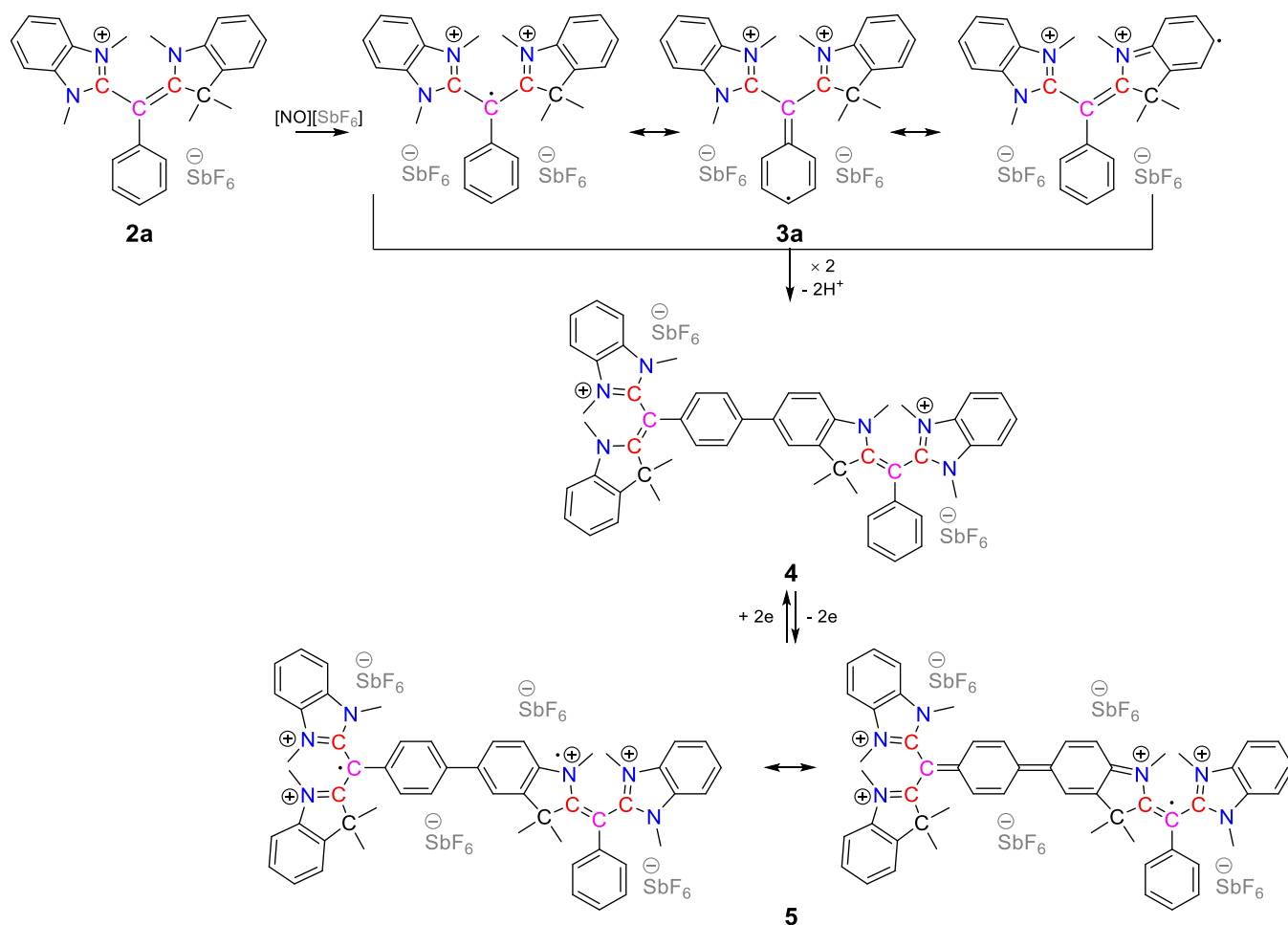


Figure 3. Spin density plots of radical-dications 3a and 3b (isovalue of 0.004) computed at the UB3LYP-D3/Def2-SVP(CH₃CN-SMD) level of theory. Two hexafluoroantimonate as counteranions and all hydrogens of both the radical-dications were omitted for clarity.

and 76% yields as yellow and orange–yellow crystalline solids, respectively (Scheme 5). The single-crystal X-ray diffraction analyses unambiguously proved their formation (Figures S89 and S90).

Cyclic voltammograms of 9a and 9b are overall chemically reversible in nature. However, in the case of 9a, from the second scan onward, two additional oxidative waves were observed at $E_{\text{pa}} = 0.36$ and 0.45 V, apart from $E_{\text{pa}} = 0.60$ V vs Fc/Fc⁺, after the follow-up reduction at $E_{\text{pc}} = 0.32$ V vs Fc/Fc⁺ (Figure 6). In the case of 9b, there was only one oxidative wave at $E_{\text{pa}} = 0.63$ V vs Fc/Fc⁺ and one reductive wave at $E_{\text{pc}} = 0.48$ V vs Fc/Fc⁺. The additional oxidative waves for 9a are most likely due to the conformational change of the NHC/

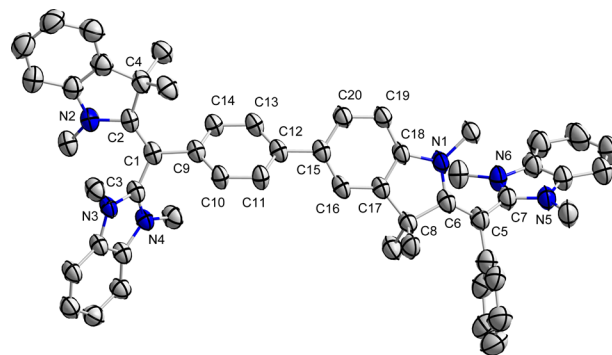
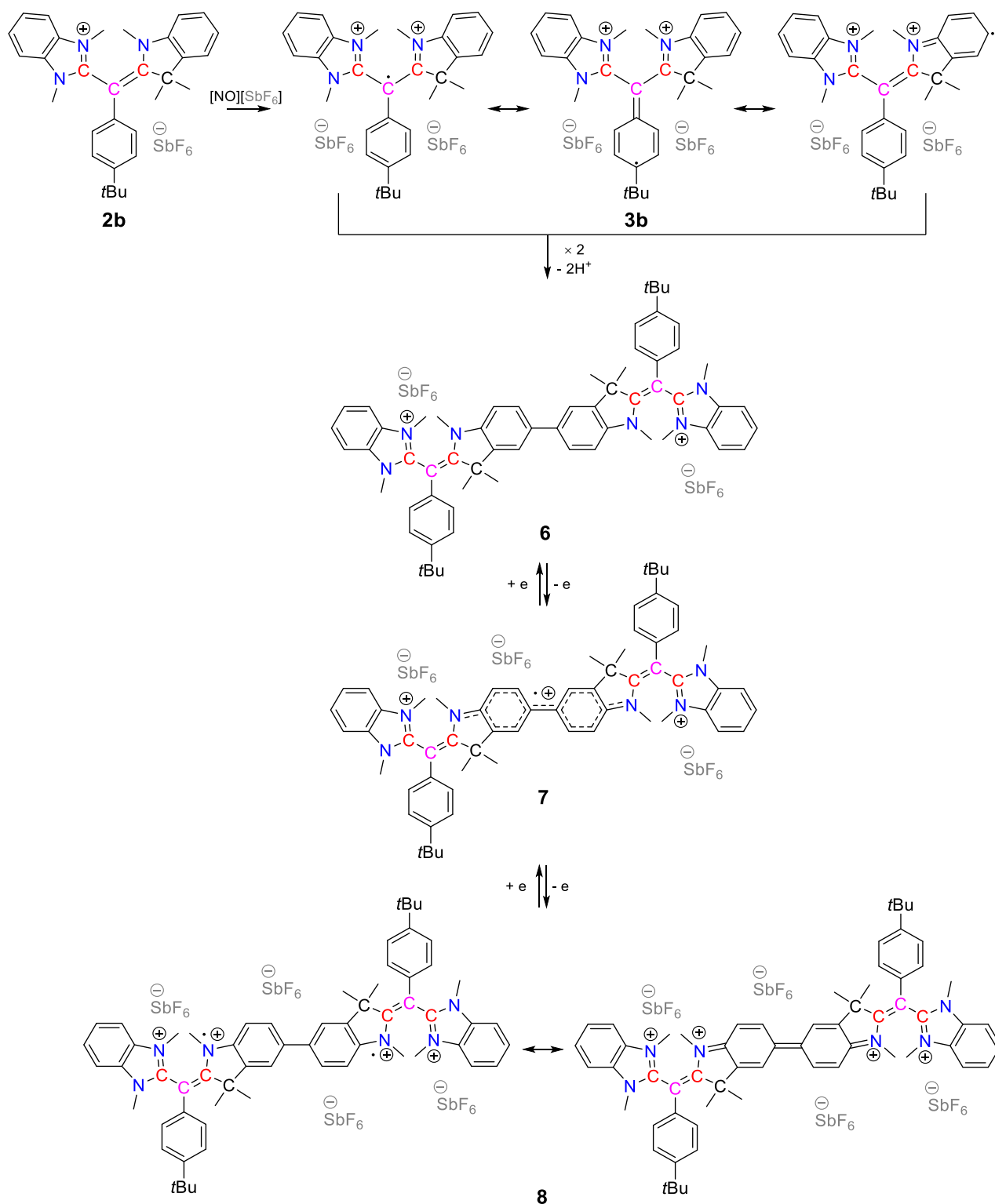


Figure 4. Molecular structure of 4 at 50% probability level. All hydrogens, counteranions, and Et₂O lattice solvent are omitted for clarity. Selected bond lengths [Å] and bond angles [°]: C1–C2 1.382(7), C1–C3 1.440(6), C1–C9 1.492(6), C12–C15 1.481(6), C5–C6 1.369(7), C5–C7 1.448(7); C5–C21 1.496(8); and C2–C1–C3 121.4(4), C2–C1–C9 123.0(4), C3–C1–C9 115.5(4), C6–C5–C7 122.0(5), C6–C5–C21 122.0(5), C7–C5–C21 115.3(4).

CAAC-carbone scaffolds during its two-electron oxidation that is reflected in their solid-state molecular structures (vide infra). However, the impact of a similar conformational change of the NHC/CAAC-carbone scaffolds is not observable in the case of 9b ($E_{\text{pa}} = 0.63$ V and $E_{\text{pc}} = 0.48$ V vs Fc/Fc⁺).

The two-electron reversible chemical oxidation of 9a/9b using two equivalents of $[\text{NO}][\text{SbF}_6]$ then led to the isolation

Scheme 4. Oxidation of 2b



of **10a/10b** as dark-red and dark-blue crystalline solids in 65 and 60% yields, respectively (Scheme 5). The analyses of the molecular structures of **9a/10a** (Figures S89 and 7 - left) revealed a decreasing C1–C5 distance from 1.513(9) to 1.380(16) Å due to the essentially quinoidal form of **10a**. The bond length alternation (BLA) value of the central *p*-phenylene bridge in **10a** is calculated to be 0.087 Å, compared to 0.10 Å in the case of the Thiele hydrocarbon.²⁰ Due to the

substantial disorder in both the cationic and the anionic parts of **10b** (Figure 7 - right), we abstain from discussing its metrical parameters. Notably, upon two-electron oxidation, we have observed a change in the NHC/CAAC-carbone scaffold's orientation in the solid-state molecular structures. In the case of **9a/9b**, the "CMe₂" units of the CAAC-motifs appear inward relative to the central π -conjugated spacer (*p*-phenylene/*p,p'*-biphenylene bridge), whereas the orientation of the "CMe₂"

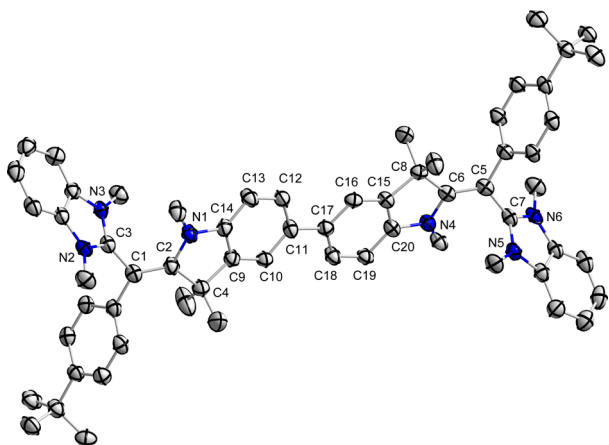


Figure 5. Molecular structure of **6** at 50% probability level. All hydrogens, counteranions, and CH₃CN lattice solvent are omitted for clarity. Selected bond lengths (Å) and bond angles (deg) for **6**: C1–C2 1.372(8), C1–C3 1.462(8), C1–C21 1.489(8), N1–C14 1.407(7), C11–C17 1.498(7); C20–N4 1.406(7); C2–C1–C3 120.6(5), C3–C1–C21 113.5(4), C2–C1–C21 125.3(5).

units of the CAAC-motifs of **10a/10b** is outward relative to the central *p*-phenylene bridge.

Bands in the UV/vis/NIR absorption spectra of compounds **10a/10b** are red-shifted ($\lambda_{\text{max}} = 497 \text{ nm}$ ($\epsilon = 38700 \text{ L mol}^{-1}\text{cm}^{-1}$) and $\lambda_{\text{max}} = 668 \text{ nm}$ ($\epsilon = 53300 \text{ L mol}^{-1}\text{cm}^{-1}$)) (Figure 8 - left) in comparison to **9a/9b** ($\lambda_{\text{max}} = 385 \text{ nm}$ ($\epsilon = 38300 \text{ L mol}^{-1}\text{cm}^{-1}$) and $\lambda_{\text{max}} = 368 \text{ nm}$ ($\epsilon = 39900 \text{ L mol}^{-1}\text{cm}^{-1}$)), respectively (Figure S79). The resonances in the ¹H NMR spectrum of **10a** are well resolved at room temperature, including those of the central *p*-phenylene ring (Figure S25). In contrast, for **10b**, the resonances of the central *p,p'*-biphenylene ring are broad at room temperature and become sharper at lower temperatures (Figure S30). This indicates the presence of a thermally excited triplet-state population at room temperature for **10b**. Indeed, compound **10a** is EPR silent, as are the Thiele's hydrocarbon²⁰ and TCNQ.²¹ Compound **10b**, in contrast, shows an increasing EPR signal intensity with rising temperature (Figure 8-center). Fitting of the temperature-dependent double-integral intensity to the Bleaney–Bowers model gives a singlet–triplet gap of $2J = -1250 \text{ cm}^{-1}$ ($\Delta E_{\text{S-T}} = -14.9 \text{ kJ/mol}$) (Figure 8 - right), suggesting a singlet ground state.

Scheme 5. Syntheses of **9a/9b** and **10a/10b**

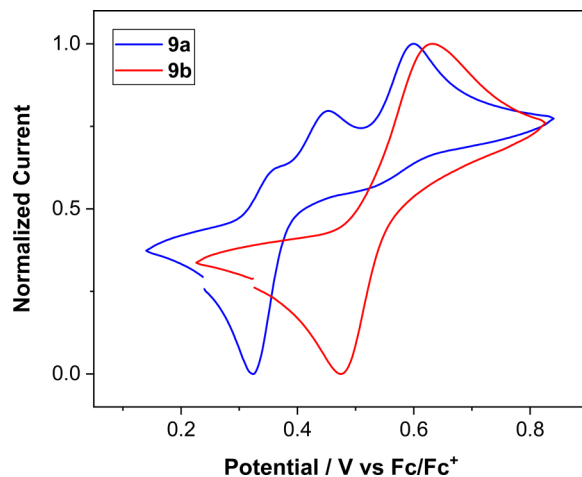
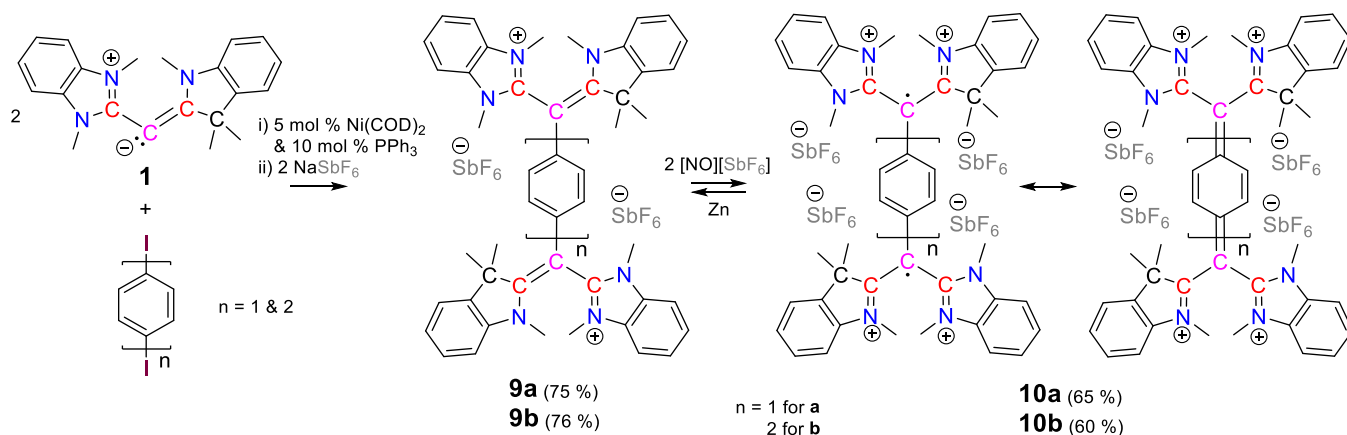


Figure 6. Cyclic voltammograms of **9a** and **9b** at a 100 mV/s scan rate in CH₃CN (0.1 mol/L Bu₄NPF₆) at room temperature.

This is also supported by the quantum chemical calculations at the UB3LYP-D3/Def2-SVP (CH₃CN-SMD) level of theory; it reveals a closed-shell singlet ground state for **10a** with $\Delta E_{\text{S-T}} = -30.9 \text{ kJ/mol}$, whereas **10b** has an open-shell singlet ground state with a close-lying triplet at $\Delta E_{\text{S-T}} = -4.9 \text{ kJ/mol}$ (Table S12).⁹ This kind of discrepancy, the calculated singlet–triplet gap, which is underestimated compared to the results obtained by VT-EPR spectroscopy ($\Delta E_{\text{S-T}} = -14.9 \text{ kJ/mol}$), has been previously known for the ionic diradicaloid systems.²² Notably, the calculated biradical character index (γ) of **10b** is 0.40, which is higher than that of **8** (0.34) and **5** (0.36).²³ Compound **10b** is quite stable, with a half-life of 19 days in CH₃CN under ambient air conditions (Figures S81 and S82); however, this is shorter than that of the oxindolyl-based Chichibabin's analogue (highly stable, no indication of degradation even after 7 days)^{19d} and sulfone-functionalized Chichibabin's analogues ($t_{1/2} = 41, 52,$ and 70 days)^{19f} but significantly longer than that of the acyclic diaminocarbene-based Chichibabin's hydrocarbon ($t_{1/2} < 1 \text{ min}$).^{19g} Compounds **10a/10b** exhibit a chemically reversible redox behavior and are reduced to **9a/9b**, respectively, upon treatment with elemental zinc, showcasing their electron-deficient nature.²⁴

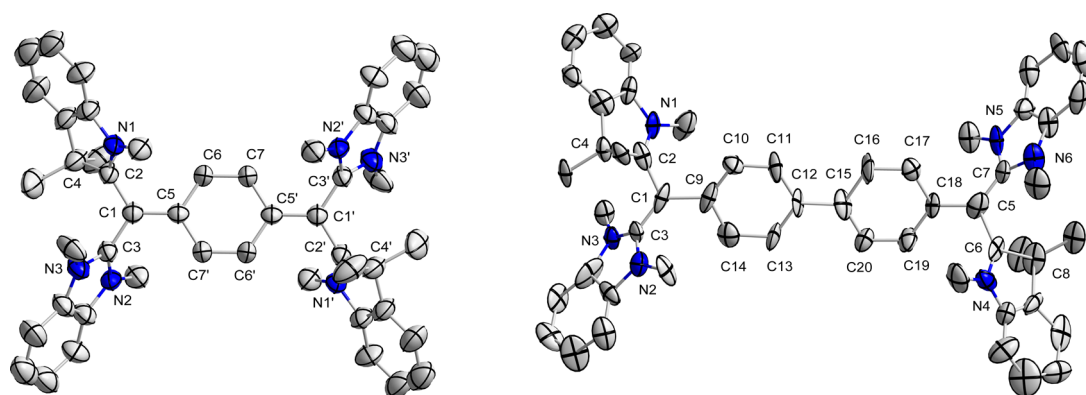


Figure 7. Molecular structures of **10a** (left) and **10b** (right) at 50 and 40% probability levels, respectively. All hydrogens and counteranions are omitted for clarity.

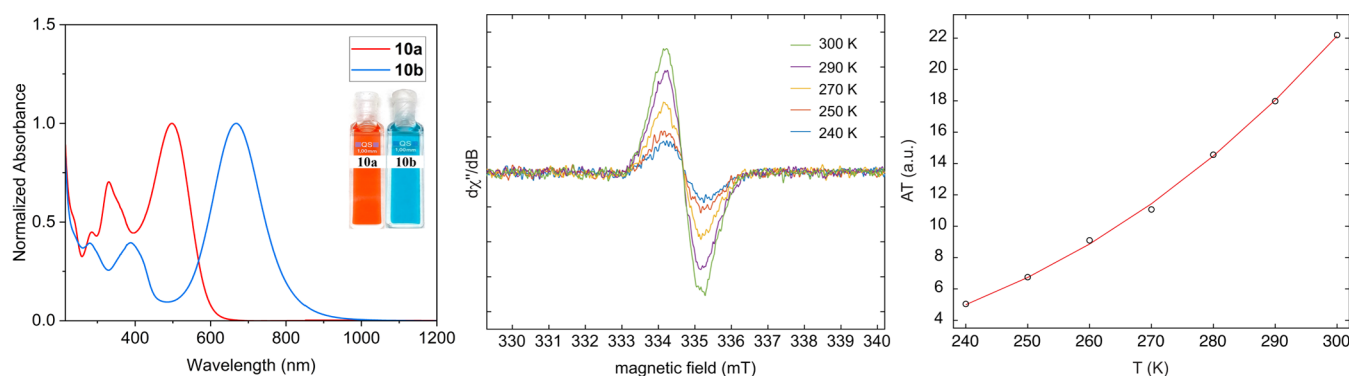


Figure 8. UV/vis/NIR spectra of **10a** and **10b** in CH_3CN at room temperature (left). Variable temperature X-band EPR spectra of **10b** in acetonitrile between 240 and 300 K (center) and temperature dependence of the double-integral EPR intensity (right). Circles (○) represent the experimental results, and the red line corresponds to the fit with the Bleaney–Bowers equation. The EPR signal is centered around a g value of 2.0027.

CONCLUSIONS

In conclusion, we have developed a nickel(0)-catalyzed cross-coupling of NHC/CAAC-carbodicarbene as a donor-stabilized atomic carbon equivalent with aryl chlorides/bromides/iodides. The resulting aryl-functionalized cationic carbodicarbene derivatives are notably electron-rich and prone to one-electron oxidation under the formation of radical-dications, which results in distinct modes of radical–radical dimerization based on the aryl substituents. Moreover, this led to the synthesis of carbon- and nitrogen/nitrogen-centered diradicaloids. Based on these findings, we have also rationally synthesized *p*-phenylene- and *p,p'*-biphenylene-bridged tetracationic carbon/carbon-centered electron-deficient diradicaloids. The electronic structure is tuned by the substantial influence of the π -conjugated spacer mirrored in the presence/absence of a triplet population. The results emphasize the unique reactivity of carbodicarbenes, specifically herein with regard to their cross-coupling with different aryl halides. The developed procedures constitute a modular methodology for the synthesis of various electron-deficient diradicaloids. This study will thus enrich the diradicaloid chemistry in general, and we are, in this context, currently engaged in developing these concepts further. Moreover, all these electron-deficient diradicaloids have potential to be used as *p*-dopants in organic semiconductors.²⁵

ASSOCIATED CONTENT

Supporting Information

The Supporting Information is available free of charge at <https://pubs.acs.org/doi/10.1021/jacs.4c08876>.

Experimental section, plots of NMR spectra for new compounds, and complete details of computational calculations (PDF)

Accession Codes

CCDC 2333307–2333314 and 2340820–2340821 contain the supplementary crystallographic data for this paper. These data can be obtained free of charge via www.ccdc.cam.ac.uk/data_request/cif, or by emailing data_request@ccdc.cam.ac.uk, or by contacting The Cambridge Crystallographic Data Centre, 12 Union Road, Cambridge CB2 1EZ, UK; fax: +44 1223 336033.

AUTHOR INFORMATION

Corresponding Authors

Gopalan Rajaraman – Department of Chemistry, Indian Institute of Technology Bombay, Mumbai 400 076, India; orcid.org/0000-0001-6133-3026; Email: rajaraman@chem.iitb.ac.in

Holger Braunschweig – Institute of Inorganic Chemistry and Institute for Sustainable Chemistry and Catalysis with Boron (ICB), Julius-Maximilians-Universität Würzburg, 97074 Würzburg, Germany; orcid.org/0000-0001-9264-1726; Email: h.braunschweig@uni-wuerzburg.de

Carola Schulzke – Institut für Biochemie, Universität Greifswald, D-17489 Greifswald, Germany; orcid.org/0000-0002-7530-539X; Email: carola.schulzke@uni-greifswald.de

Anukul Jana – Tata Institute of Fundamental Research Hyderabad, Hyderabad 500046, India; orcid.org/0000-0002-1657-1321; Email: ajana@tifrh.res.in

Authors

Vasu Malhotra – Tata Institute of Fundamental Research Hyderabad, Hyderabad 500046, India; orcid.org/0000-0002-6165-5188

Benedict J. Elvers – Institut für Biochemie, Universität Greifswald, D-17489 Greifswald, Germany; orcid.org/0000-0002-4627-6905

Ramapada Dolai – Tata Institute of Fundamental Research Hyderabad, Hyderabad 500046, India

Nicolas Chrysochos – Tata Institute of Fundamental Research Hyderabad, Hyderabad 500046, India

Siva Sankar Murthy Bandaru – Institut für Biochemie, Universität Greifswald, D-17489 Greifswald, Germany; orcid.org/0000-0003-4294-8521

Tejaswinee Gangber – Tata Institute of Fundamental Research Hyderabad, Hyderabad 500046, India

Neethinathan Johnee Britto – Department of Chemistry, Indian Institute of Technology Bombay, Mumbai 400 076, India

Ivo Krummenacher – Institute of Inorganic Chemistry and Institute for Sustainable Chemistry and Catalysis with Boron (ICB), Julius-Maximilians-Universität Würzburg, 97074 Würzburg, Germany; orcid.org/0000-0001-9537-1506

Complete contact information is available at:

<https://pubs.acs.org/10.1021/jacs.4c08876>

Notes

The authors declare the following competing financial interest(s): We are working to file a patent related to the findings of this manuscript.

ACKNOWLEDGMENTS

We acknowledge generous support of the Department of Atomic Energy, Government of India, under Project Identification No. RTI 4007 and SERB (CRG/2023/004314), India. G.R. would like to thank SERB (SB/SJF/2019-20/12 and CRG/2022/001697) for funding.

DEDICATION

Dedicated to Indian Chemical Society Centenary.

REFERENCES

- (1) Selected reviews are: (a) Biffis, A.; Centomo, P.; Del Zotto, A.; Zecca, M. Pd Metal Catalysts for Cross-Couplings and Related Reactions in the 21st Century: A Critical Review. *Chem. Rev.* **2018**, *118*, 2249–2295. (b) Suzuki, A. Cross-Coupling Reactions of Organoboranes: An Easy Way to Construct C–C Bonds (Nobel Lecture). *Angew. Chem., Int. Ed.* **2011**, *50*, 6722–6737. (c) Magano, J.; Dunetz, J. R. Large-Scale Applications of Transition Metal-Catalyzed Couplings for the Synthesis of Pharmaceuticals. *Chem. Rev.* **2011**, *111*, 2177–2250. (d) Corbet, J.-P.; Mignani, G. Selected Patented Cross-Coupling Reaction Technologies. *Chem. Rev.* **2006**, *106*, 2651–2710.
- (2) Selected reviews are: (a) Dong, Z.; Ren, Z.; Thompson, S. J.; Xu, Y.; Dong, G. Transition-Metal-Catalyzed C–H Alkylation Using Alkenes. *Chem. Rev.* **2017**, *117*, 9333–9403. (b) Boyarskiy, V. P.;

Ryabukhin, D. S.; Bokach, N. A.; Vasilyev, A. V. Alkenylation of Arenes and Heteroarenes with Alkynes. *Chem. Rev.* **2016**, *116*, 5894–5986. (c) Chinchilla, R.; Nájera, C. Recent Advances in Sonogashira Reactions. *Chem. Soc. Rev.* **2011**, *40*, 5084–5121.

(3) (a) Ghadwal, R. S.; Reichmann, S. O.; Herbst-Irmer, R. Palladium-Catalyzed Direct C2-Arylation of an *N*-Heterocyclic Carbene: An Atom-Economic Route to Mesoionic Carbene Ligands. *Chem.-Eur. J.* **2015**, *21*, 4247–4251. (b) Ho, N. K. T.; Neumann, B.; Stammler, H.-G.; Menezes da Silva, V. H.; Watanabe, D. G.; Braga, A. A. C.; Ghadwal, R. S. Nickel-Catalyzed Direct C2-Arylation of *N*-Heterocyclic Carbenes. *Dalton Trans.* **2017**, *46*, 12027–12031. (c) Rottschäfer, D.; Neumann, B.; Stammler, H.-G.; van Gestel, M.; Andrada, D. M.; Ghadwal, R. S. Crystalline Radicals Derived from Classical *N*-Heterocyclic Carbenes. *Angew. Chem., Int. Ed.* **2018**, *57*, 4765–4768.

(4) (a) Tonner, R.; Frenking, G. C(NHC)₂: Divalent Carbon(0) Compounds with *N*-Heterocyclic Carbene Ligands-Theoretical Evidence for a Class of Molecules with Promising Chemical Properties. *Angew. Chem., Int. Ed.* **2007**, *46*, 8695–8698. (b) Tonner, R.; Oxler, F.; Neumüller, B.; Petz, W.; Frenking, G. Carbodiphosphoranes: The Chemistry of Divalent Carbon(0). *Angew. Chem., Int. Ed.* **2006**, *45*, 8038–8042.

(5) Selected references are: (a) Dyker, C. A.; Lavallo, V.; Donnadiou, B.; Bertrand, G. Synthesis of an Extremely Bent Acyclic Allene (A “Carbodicarbene”): A Strong Donor Ligand. *Angew. Chem., Int. Ed.* **2008**, *47*, 3206–3209. (b) Fürstner, A.; Alcarazo, M.; Goddard, R.; Lehmann, C. W. Coordination Chemistry of Ene-1,1-diamines and a Prototype “Carbodicarbene”. *Angew. Chem., Int. Ed.* **2008**, *47*, 3210–3214. (c) Su, W.; Pan, S.; Sun, X.; Wang, S.; Zhao, L.; Frenking, G.; Zhu, C. Double Dative Bond between Divalent Carbon(0) and Uranium. *Nat. Commun.* **2018**, *9*, 4997. (d) Aweke, B. S.; Yu, C.-H.; Zhi, M.; Chen, W.-C.; Yap, G. P. A.; Zhao, L.; Ong, T.-G. A Bis-(Carbene) Pincer Ligand and Its Coordinative Behavior toward Multi-Metallic Configurations. *Angew. Chem., Int. Ed.* **2022**, *61*, e202201884. (e) Hollister, K. K.; Molino, A.; Breiner, G.; Walley, J. E.; Wentz, K. E.; Conley, A. M.; Dickie, D. A.; Wilson, D. J. D.; Gilliard, R. J., Jr. Air-Stable Thermoluminescent Carbodicarbene-Borafluorenum Ions. *J. Am. Chem. Soc.* **2022**, *144*, 590–598.

(6) Dolai, R.; Kumar, R.; Elvers, B. J.; Pal, P. K.; Joseph, B.; Sikari, R.; Nayak, M. K.; Maiti, A.; Singh, T.; Chrysochos, N.; Jayaraman, A.; Krummenacher, I.; Mondal, J.; Priyakumar, U. D.; Braunschweig, H.; Yildiz, C. B.; Schulzke, C.; Jana, A. Carbodicarbenes and Striking Redox Transitions of Their Conjugate Acids: Influence of NHC versus CAAC as Donor Substituents. *Chem.-Eur. J.* **2023**, *29*, e202202888.

(7) (a) Himmel, D.; Krossing, I.; Schnepf, A. Dative Bonds in Main-Group Compounds: A Case for Fewer Arrows! *Angew. Chem., Int. Ed.* **2014**, *53*, 370–374. (b) Frenking, G. Dative Bonds in Main-Group Compounds: A Case for More Arrows! *Angew. Chem., Int. Ed.* **2014**, *53*, 6040–6046.

(8) (a) Lavallo, V.; Canac, Y.; Donnadiou, B.; Schoeller, W. W.; Bertrand, G. CO Fixation to Stable Acyclic and Cyclic Alkyl Amino Carbenes: Stable Amino Ketenes with a Small HOMO-LUMO Gap. *Angew. Chem., Int. Ed.* **2006**, *45*, 3488–3491. (b) Frey, G. D.; Lavallo, V.; Donnadiou, B.; Schoeller, W. W.; Bertrand, G. Facile Splitting of Hydrogen and Ammonia by Nucleophilic Activation at a Single Carbon Center. *Science* **2007**, *316*, 439–441.

(9) See the [Supporting Information](#) for experimental details, analytical data, NMR spectra, UV/Vis/NIR absorption spectra, electrochemistry details, X-ray crystallographic details, details of EPR spectroscopy, and details of quantum chemical calculations.

(10) The cyclic voltammogram of **2a** is the average of the second and third scans at 100 mV/s at room temperature, where the presence of shoulder peaks at $E_{pc} = 0.53$ and $E_{pa} = 0.60$ V vs Fc/Fc⁺ most likely represent the redox behavior of in situ formed **4**, originating from the oxidation of **2a**. In the first cycle, no such shoulder peak is observed at $E_{pa} = 0.60$ V vs Fc/Fc⁺ (Figure S94).

(11) See the related heteroleptic dimerization based on triphenylmethyl radical and related system: (a) Lankamp, H.; Nauta, W. T.;

MacLean, C. A New Interpretation of the Monomer-Dimer Equilibrium of Triphenylmethyl- and Alkylsubstituted-Diphenyl Methyl-Radicals in Solution. *Tetrahedron Lett.* **1968**, *9*, 249–254.

(b) Mandal, D.; Sobottka, S.; Dolai, R.; Maiti, A.; Dhara, D.; Kalita, P.; Narayanan, R. S.; Chandrasekhar, V.; Sarkar, B.; Jana, A. Direct access to 2-aryl substituted pyrrolinium salts for carbon centre based radicals without pyrrolidine-2-ylidene alias cyclic(alkyl)(amino)-carbene (CAAC) as a precursor. *Chem. Sci.* **2019**, *10*, 4077–4081.

(12) Connelly, N. G.; Geiger, W. E. Chemical Redox Agents for Organometallic Chemistry. *Chem. Rev.* **1996**, *96*, 877–910.

(13) Compound **5** represents the class of not-yet-isolated carbon/nitrogen-centered heteronuclear diradicaloids.²⁶ Indeed, it exhibits triplet population at room temperature and the variable temperature-EPR study reveals a singlet ground state with $\Delta E_{S-T} = -8.7$ kJ/mol (Figure S132). This is also supported by the quantum chemical calculations which suggest closed-shell singlet as the ground state with singlet-triplet gap $\Delta E_{S-T} = -8.6$ kJ/mol (Table S12).⁹

(14) See the related dimerization based on triarylamine radical-cation: Zheng, X.; Wang, X.; Qiu, Y.; Li, Y.; Zhou, C.; Sui, Y.; Li, Y.; Ma, J.; Wang, X. One-Electron Oxidation of an Organic Molecule by B(C₆F₅)₃; Isolation and Structures of Stable Non-para-Substituted Triarylamine Cation Radical and Bis(Triarylamine) Dication Diradicaloid. *J. Am. Chem. Soc.* **2013**, *135*, 14912–14915.

(15) (a) Müller, E.; Moosmayer, A.; Rieker, A.; Scheffler, K. Sesquioxanthryl, ein "ebenes" triarylmethylradikal. *Tetrahedron Lett.* **1967**, *8*, 3877–3880. (b) Staab, H. A.; Bretschneider, H.; Brunner, H. Struktur Der Triarylmethyl-dimeren. *Chem. Ber.* **1970**, *103*, 1101–1106. (c) Kahr, B.; Van Engen, D.; Mislow, K. Length of the Ethane Bond in Hexaphenylethane and Its Derivatives. *J. Am. Chem. Soc.* **1986**, *108*, 8305–8307. (d) Grimme, S.; Schreiner, P. R. Steric Crowding Can Stabilize a Labile Molecule: Solving the Hexaphenylethane Riddle. *Angew. Chem., Int. Ed.* **2011**, *50*, 12639–12642. (e) Jang, S.-H.; Gopalan, P.; Jackson, J. E.; Kahr, B. Jacobson and Heintschel Peroxides. *Angew. Chem., Int. Ed.* **1994**, *33*, 775–777. (f) Yokoi, H.; Hiroto, S.; Shinokubo, H. Reversible σ -Bond Formation in Bowl-Shaped π -Radical Cations: The Effects of Curved and Planar Structures. *J. Am. Chem. Soc.* **2018**, *140*, 4649–4655. (g) Takemasa, Y.; Nozaki, K. Hexakispyrazolylethane: New Strategy for Stabilization of Hexaarylethane. *Chem.-Eur. J.* **2024**, *30*, e202303575.

(16) Compound **8** represents the nitrogen analogue of Chichibabin's hydrocarbon.²⁷ It exhibits triplet population at room temperature, and the variable temperature-EPR study reveals a singlet ground state with $\Delta E_{S-T} = -10.9$ kJ/mol (Figure S134). This is also supported by the quantum chemical calculations which suggest singlet as the ground state with an underestimated²² close-lying triplet state at $\Delta E_{S-T} = -3.7$ kJ/mol (Table S12).⁹

(17) These are rarely described in the literature but not unprecedented; see for instance: Haase, W. Die Kristall- Und Molekülstruktur von Dicäsium- μ -oxo-decafluorodiantimonat, Cs₂[Sb₂F₁₀O]. *Chem. Ber.* **1973**, *106*, 41–47. In the crystal structure of compound **8**, two [Sb₂F₁₀O]²⁻ dianions were found to be the counteranions.

(18) Selected references are: (a) Thiele, J.; Balhorn, H. Ueber einen chinoiden Kohlenwasserstoff. *Ber. Dtsch. Chem. Ges.* **1904**, *37*, 1463–1470. (b) Okamoto, Y.; Tanioka, M.; Muranaka, A.; Miyamoto, K.; Aoyama, T.; Ouyang, X.; Kamino, S.; Sawada, D.; Uchiyama, M. Stable Thiele's Hydrocarbon Derivatives Exhibiting near-Infrared Absorption/Emission and Two-Step Electrochromism. *J. Am. Chem. Soc.* **2018**, *140*, 17857–17861. (c) Maiti, A.; Stubbe, J.; Neuman, N. I.; Kalita, P.; Duari, P.; Schulzke, C.; Chandrasekhar, V.; Sarkar, B.; Jana, A. CAAC-Based Thiele and Schlenk Hydrocarbons. *Angew. Chem., Int. Ed.* **2020**, *59*, 6729–6734. (d) Mahata, A.; Chandra, S.; Maiti, A.; Rao, D. K.; Yildiz, C. B.; Sarkar, B.; Jana, A. α,α' -Diamino-*p*-Quinodimethanes with Three Stable Oxidation States. *Org. Lett.* **2020**, *22*, 8332–8336. (e) Jana, S.; Elvers, B. J.; Patsch, S.; Sarkar, P.; Krummenacher, I.; Nayak, M. K.; Maiti, A.; Chrysochos, N.; Pati, S. K.; Schulzke, C.; Braunschweig, H.; Yildiz, C. B.; Jana, A. Air and Moisture Stable *para*- and *ortho*-Quinodimethane Derivatives Derived from *bis-N*-Heterocyclic Olefins. *Org. Lett.* **2023**, *25*, 1799–1804.

(f) Punzi, A.; Dai, Y.; Dibenedetto, C. N.; Mesto, E.; Schingaro, E.; Ullrich, T.; Striccoli, M.; Guldi, D. M.; Negri, F.; Farinola, G. M.; Blasi, D. Dark State of the Thiele Hydrocarbon: Efficient Solvatochromic Emission from a Nonpolar Centrosymmetric Singlet Diradicaloid. *J. Am. Chem. Soc.* **2023**, *145*, 20229–20241. (g) Liu, C.-H.; He, Z.; Ruchlin, C.; Che, Y.; Somers, K.; Perepichka, D. F. Thiele's Fluorocarbons: Stable Diradicaloids with Efficient Visible-to-Near-Infrared Fluorescence from a Zwitterionic Excited State. *J. Am. Chem. Soc.* **2023**, *145*, 15702–15707. (h) Banachowicz, P.; Das, M.; Kruczala, K.; Siczek, M.; Sojka, Z.; Kijewska, M.; Pawlicki, M. Breaking Global Diatropic Current to Tame Diradicaloid Character: Thiele's Hydrocarbon Under Macrocyclic Constraints. *Angew. Chem., Int. Ed.* **2024**, *63*, e202400780.

(19) Selected references are: (a) Tschitschibabin, A. E. Über einige phenylierte Derivate des *p*, *p*-Ditolyls. *Ber. Dtsch. Chem. Ges.* **1907**, *40*, 1810–1819. (b) Zeng, Z.; Sung, Y. M.; Bao, N.; Tan, D.; Lee, R.; Zafra, J. L.; Lee, B. S.; Ishida, M.; Ding, J.; López Navarrete, J. T.; Li, Y.; Zeng, W.; Kim, D.; Huang, K.-W.; Webster, R. D.; Casado, J.; Wu, J. Stable Tetrabenzo-Chichibabin's Hydrocarbons: Tunable Ground State and Unusual Transition between Their Closed-Shell and Open-Shell Resonance Forms. *J. Am. Chem. Soc.* **2012**, *134*, 14513–14525. (c) Sbgoud, K.; Mamada, M.; Marrot, J.; Tokito, S.; Yassar, A.; Frigoli, M. Diindeno[1,2-*b*:2',1'-*n*]Perylene: A Closed Shell Related Chichibabin's Hydrocarbon, the Synthesis, Molecular Packing, Electronic and Charge Transport Properties. *Chem. Sci.* **2015**, *6*, 3402–3409. (d) Wang, J.; Xu, X.; Phan, H.; Herng, T. S.; Gopalakrishna, T. Y.; Li, G.; Ding, J.; Wu, J. Stable Oxindolyl-Based Analogues of Chichibabin's and Müller's Hydrocarbons. *Angew. Chem., Int. Ed.* **2017**, *56*, 14154–14158. (e) Majewski, M. A.; Chmielewski, P. J.; Chien, A.; Hong, Y.; Lis, T.; Witwicki, M.; Kim, D.; Zimmerman, P. M.; Stępień, M. 5,10-Dimesityldiindeno[1,2-*a*:2',1'-*i*]Phenanthrene: A Stable Biradicaloid Derived from Chichibabin's Hydrocarbon. *Chem. Sci.* **2019**, *10*, 3413–3420. (f) Zhou, Z.; Yang, K.; He, L.; Wang, W.; Lai, W.; Yang, Y.; Dong, Y.; Xie, S.; Yuan, L.; Zeng, Z. Sulfone-Functionalized Chichibabin's Hydrocarbons: Stable Diradicaloids with Symmetry Breaking Charge Transfer Contributing to NIR Emission beyond 900 Nm. *J. Am. Chem. Soc.* **2024**, *146*, 6763–6772. (g) Maiti, A.; Chandra, S.; Sarkar, B.; Jana, A. Acyclic Diaminocarbene-Based Thiele, Chichibabin, and Müller Hydrocarbons. *Chem. Sci.* **2020**, *11*, 11827–11833. (h) Chang, X.; Arnold, M. E.; Blinder, R.; Zolg, J.; Wischnat, J.; van Slageren, J.; Jelezko, F.; Kuehne, A. J. C.; von Delius, M. A Stable Chichibabin Diradicaloid with Near-Infrared Emission. *Angew. Chem., Int. Ed.* **2024**, *63*, e202404853.

(20) Montgomery, L. K.; Huffman, J. C.; Jurczak, E. A.; Grendze, M. P. The molecular structures of Thiele's and Chichibabin's hydrocarbons. *J. Am. Chem. Soc.* **1986**, *108*, 6004–6011.

(21) Acker, D. S.; Hertler, W. R. Substituted Quinodimethans I. Preparation and Chemistry of 7,7,8,8-Tetracyanoquinodimethan. *J. Am. Chem. Soc.* **1962**, *84*, 3370–3374.

(22) (a) Chen, C.; Ruan, H.; Feng, Z.; Fang, Y.; Tang, S.; Zhao, Y.; Tan, G.; Su, Y.; Wang, X. Crystalline Diradical Dianions of Pyrene-Fused Azaacenes. *Angew. Chem., Int. Ed.* **2020**, *59*, 11794–11799. (b) Maiti, A.; Zhang, F.; Krummenacher, I.; Bhattacharyya, M.; Mehta, S.; Moos, M.; Lambert, C.; Engels, B.; Mondal, A.; Braunschweig, H.; Ravat, P.; Jana, A. Anionic Boron- and Carbon-Based Hetero-Diradicaloids Spanned by a *p*-Phenylene Bridge. *J. Am. Chem. Soc.* **2021**, *143*, 3687–3692.

(23) (a) Yamaguchi, K. The Electronic Structures of Biradicals in the Unrestricted Hartree-Fock Approximation. *Chem. Phys. Lett.* **1975**, *33*, 330–335. (b) Domínguez, I. B.; Canola, S.; Jolín, V. H.; Navarrete, J. T. L.; García, J. C. S.; Negri, F.; Delgado, M. C. R. Tuning the Diradical Character of Indolocarbazoles: Impact of Structural Isomerism and Substitution Position. *J. Phys. Chem. Lett.* **2022**, *13*, 6003–6010. (c) Bodzioch, A.; Obijalska, E.; Jakubowski, R.; Celeda, M.; Gardias, A.; Trzybiński, D.; Tokarz, P.; Szczytko, J.; Woźniak, K.; Kaszyński, P. Electronic and Magnetic Interactions in 6-Oxoverdazyl Diradicals: Connection through N(1) vs C(3) Revisited. *J. Org. Chem.* **2024**, *89*, 6306–6321.

(24) The electron-deficient carbon/carbon-centered diradicaloids are mostly known with cyano-substituents, such as in: Zeng, Z.; Ishida, M.; Zafra, J. L.; Zhu, X.; Sung, Y. M.; Bao, N.; Webster, R. D.; Lee, B. S.; Li, R.-W.; Zeng, W.; Li, Y.; Chi, C.; López Navarrete, J. T.; Ding, J.; Casado, J.; Kim, D.; Wu, J. Pushing Extended *p*-Quinodimethanes to the Limit: Stable Tetracyano-Oligo(*N*-Annulated Perylene)Quinodimethanes with Tunable Ground States. *J. Am. Chem. Soc.* **2013**, *135*, 6363–6371.

(25) Suh, E. H.; Kim, S. B.; Jung, J.; Jang, J. Extremely Electron-Withdrawing Lewis-Paired CN Groups for Organic *p*-Dopants. *Angew. Chem., Int. Ed.* **2023**, *62*, e202304245.

(26) Bobet, A.; Cuadrado, A.; Fajari, L.; Sirés, I.; Brillas, E.; Almajano, M. P.; Jankauskas, V.; Velasco, D.; Juliá, L. Bipolar Charge Transport in Organic Electron Donor-Acceptor Systems with Stable Organic Radicals as Electron-Withdrawing Moieties. *J. Phys. Org. Chem.* **2019**, *32*, e3974.

(27) (a) Kamada, K.; Fuku-en, S.-I.; Minamide, S.; Ohta, K.; Kishi, R.; Nakano, M.; Matsuzaki, H.; Okamoto, H.; Higashikawa, H.; Inoue, K.; Kojima, S.; Yamamoto, Y. Impact of Diradical Character on Two-Photon Absorption: Bis(Acridine) Dimers Synthesized from an Allenic Precursor. *J. Am. Chem. Soc.* **2013**, *135*, 232–241. (b) Tan, G.; Wang, X. Isolable Bis(triarylamine) Dications: Analogues of Thiele's, Chichibabin's, and Müller's Hydrocarbons. *Acc. Chem. Res.* **2017**, *50*, 1997–2006.